Available online at www.CivileJournal.org

Civil Engineering Journal

(E-ISSN: 2476-3055; ISSN: 2676-6957)

Vol. 12, No. 05, May, 2026

Calculation of Active Earth Pressure in Cohesive Soils Based on Slope Stability

Shi-Wei Wu [1], Tao Yang [1], De-Pei Zhou [1*], Han-Qing Teng [1], Zhe Zhang [1]

[1] *Department of Civil Engineering, Southwest Jiaotong University, Chengdu 610031, China*.

Received 16 December 2025; Revised 11 April 2026; Accepted 15 April 2026; Published 01 May 2026

Abstract

Extensive engineering experience has shown that the stability of cohesive soil slopes behind retaining walls has a significant impact on earth pressure. This manuscript investigates the influence of the stability of a cohesive soil slope behind a retaining wall on earth pressure. To elucidate the patterns of how slope stability affects earth pressure, first, an analysis of the interaction mechanism between the wall and the slope was carried out to clarify the mechanical behavior of clay soil pressure. Secondly, based on the assumption of plane slip damage and limit equilibrium condition, the active earth pressure calculation equation for cohesive soil considering slope stability was proposed. Thirdly, based on the proposed equation, this manuscript analyzed the influence of various slope parameters on earth pressure and proposed a method for determining the most dangerous slip surface and inclination angle of a slope. Finally, the validity of this equation was verified through a large number of arithmetic examples. These results can be conveniently and easily applied to the calculation of earth pressures in slopes with clayey and sandy soil and also provide a new approach and reference for gaining a deeper understanding of the complex mechanical behavior of earth pressure in cohesive soils.

Keywords: Slope Stability; Cohesive Soil; Active Earth Pressure; Plane Sliding; The Most Dangerous Slip Surface.

1. Introduction

When a retaining wall moves away from the soil, causing the soil behind the wall to reach a state of limit equilibrium, the earth pressure acting on the wall is called active earth pressure [1, 2]. The Coulomb theory and the Rankine theory are commonly used to calculate earth pressure [3-5]. However, when applying these two methods, certain prerequisites must be met in the external environment, such as smooth retaining walls or non-cohesive soil slopes, and therefore the calculated earth pressure results may contain some error [6, 7]. To address this issue, scholars worldwide have proposed various solutions [8-10]. A series of earth‑pressure calculation equations was derived based on the plane‑slip failure hypothesis and the limit‑equilibrium condition, and the special cases of these equations correspond to the results of Coulomb and Rankine theories [11, 12]. Terzaghi [13] proposed a graphical method for determining lateral earth pressures in cohesive soils by plotting multiple Mohr circles [14, 15]. At the same time, the method was further developed and simplified, and analytical expressions for the earth‑pressure coefficients were derived [16-18].

Although there is already a wealth of well-established research on the calculation of earth pressures on retaining walls both domestically and internationally [19-21], existing research has not yet addressed the impact of the stability of the slope behind a retaining wall on earth pressure. Therefore, further study is warranted. This manuscript investigates the influence of slope stability behind retaining walls on earth pressure in cohesive soil slopes; the workflow is shown

* Corresponding author: 18328073568@163.com

https://doi.org/10.28991/CEJ-2026-012-05-010

in Figure 1. Based on the plane slip failure hypothesis and limit equilibrium conditions, an equation for calculating active earth pressure in cohesive soil that accounts for slope stability was derived. Using this equation, this manuscript reveals the relationship between slope stability and earth pressure, provides a recommended method for determining the most dangerous slip plane and its inclination angle, and identifies the influence of various slope parameters on earth pressure. These findings facilitate straightforward calculations of earth pressure in slopes with clayey and sandy soil, while also offering a new approach and reference for deepening the understanding of the complex mechanical behavior of earth pressure in cohesive soils.

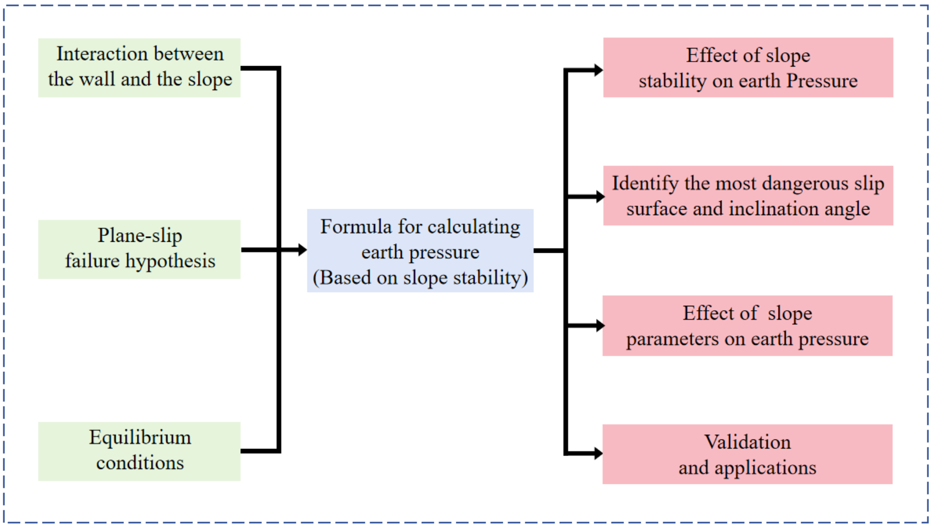

Figure 1. Workflow diagram

2. Derivation of Earth Pressure Calculation Equations

2.1. Interaction Mechanism Between Walls and Slopes

When slope instability leads to sliding failure, the slip surface may exhibit complex forms such as arcs, broken lines, or planes. For illustrative purposes, this paper assumes a planar slip surface and studies the retaining wall system model shown in Figure 2. The focus is on investigating the interaction mechanism between the wall and the slope behind it. This analysis proposes an earth pressure calculation equation that accounts for slope stability behind the wall, revealing the influence of slope stability on earth pressure.

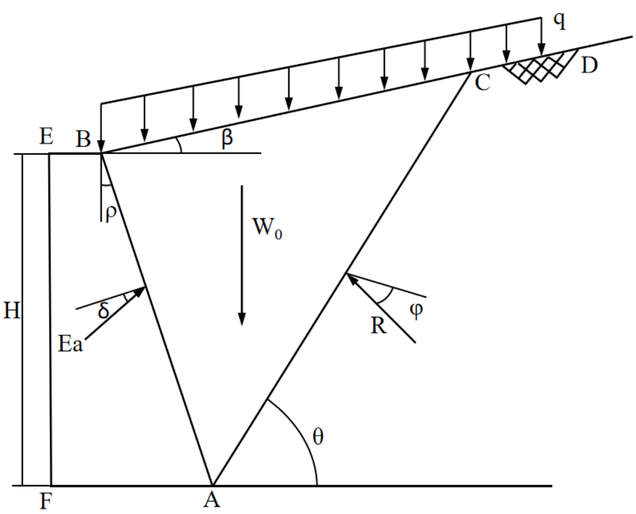

Figure 2. The model of wall and soil system

Figure 2 depicts a wall-soil system model composed of retaining wall ABEF and the slope ABD behind the wall. The wall and soil interact with each other. It is currently widely accepted that active earth pressure is the pressure exerted on the wall when the soil reaches an active limit equilibrium state due to the displacement caused by the wall. The relationship between the two is that wall displacement induces slope instability. If the portion of the slope behind the wall exhibits a tendency to slide downward along any slip surface AC with inclination angle θ, the sliding mass ABC will exert pressure on the wall. This results in an earth pressure E acting on the wall, which simultaneously provides an equal counterforce to maintain static equilibrium. In other words, although the wall is subjected to the force exerted by the sliding mass, it can generate sufficient resistance to prevent the progression of the sliding tendency, thereby maintaining its own equilibrium state. The slope behind the wall may exhibit different slip surfaces due to varying inclination angles θ of the slip surface AC, resulting in differing earth pressures exerted on the wall. Among these, the slip surface with inclination angle θ_r corresponds to the slip body exerting the maximum earth pressure *Ea* on the wall. This slip surface represents the most potentially hazardous slip surface within the slope. If the wall can still provide sufficient resistance to balance *Ea* at this point, equilibrium is maintained even if the wall exhibits displacement tendencies. Otherwise, the sliding tendency of the slip block will continue, causing excessive wall movement and damage. This state of equilibrium is termed the static limit equilibrium state, where 'limit' indicates that the earth pressure *E* reaches its maximum value *Ea*, where *Ea* is the active earth pressure. Below, we explore the equation for calculating *Ea* based on this interaction mechanism between the wall and the slope.

2.2. Derivation of the Active Earth Pressure Equation for Cohesive Soils Based on Slope Stability

The model in Figure 1 involves eight slope parameters: slope height *H*, vertical inclination angle ρ of the wall surface (wall-soil contact surface) AB (positive for downward-sloping walls, negative for upward-sloping walls), friction angle δ between the wall and soil, horizontal inclination angle β of the crest surface BD, unit weight γ of cohesive soil, cohesion *C*, internal friction angle φ, and uniformly distributed gravity load *q* on the crest. When the sliding body interacts with the wall to reach a state of static equilibrium, assume that the most dangerous slip plane is AC with its inclination angle θ_r. The forces acting on the sliding body ABC include earth pressure *Ea*, the body's self-weight W_0, and the gravitational load W_q generated by the crown load *q*. Decomposing these forces along the slip plane AC direction, according to slope stability analysis methods, the resisting force *P* and the sliding force *N* in the slip plane AC direction must be in a state of limit equilibrium (i.e., they should be equal). Therefore:

$$\begin{aligned} &P = W cos\theta_r tan\varphi + C \cdot AC + E_a[sin(\theta_r - \varepsilon)\, tan\varphi + cos(\theta_r - \varepsilon)] \\ &N = W sin\theta_r \\ &P = N \end{aligned} \tag{1}$$

where, *W* is gravitational load, $W = W_0 + W_q = \frac{\gamma H^2}{2}(1 + \frac{2qn}{\gamma H}) * \frac{\cos(\rho-\beta)\cos(\theta_r-\rho)}{\cos^2\rho sin(\theta_r-\beta)}$; *Ea* is Earth pressure; *P* is Slip resistance in the AC direction; *N* is Downward force in the AC direction; *q* is Uniformly distributed dead load; *C* is Cohesion; γ is Soil density; *AC* is Sliding surface length, $AC = \frac{H\cos(\rho-\beta)}{\cos\rho\cdot sin(\theta-\beta)}$; *AB* is Wall-soil contact surface; *H* is Slope height; θ_r is Slide angle; ρ is Vertical angle at the wall-soil interface AB; δ is Angle of friction between the wall and soil; φ is Internal friction angle; β is The horizontal slope angle of the roof surface BD; $\varepsilon = \delta + \rho$.

In the above equation, n is the influence coefficient of the load q, $n = \frac{cos\beta cos\rho}{cos(\rho-\beta)}$. Solving for earth pressure *Ea* from Equation 1 yields the following expression after calculation:

$$\begin{aligned} &E_a = \frac{W\sin\theta_r\cos\varphi(1-F)}{\cos(\theta_r-\omega)} \\ &F = \frac{\tan\varphi}{\tan\theta_r} + \frac{m\cos\rho}{\cos(\theta_r-\rho)\sin\theta_r} \end{aligned} \tag{2}$$

where, *F* is Safety factor when the slope behind the wall is in a state of ultimate equilibrium; *m* is Bond strength influence coefficient, $m = \frac{2C}{\gamma H+2qn}$; $\omega = \varphi + \varepsilon$.

Substituting the equations for *W* and *F* into Equation 2 yields another expression for *Ea*:

$$\begin{aligned} &E_a = \frac{\gamma H^2}{2}(1 + \frac{2qn}{\gamma H})K_a \\ &K_a = \frac{\cos(\rho-\beta)}{\cos^2\rho} * \frac{\sin(\theta_r-\varphi)\cos(\theta_r-\rho) - m\cos\rho\cos\varphi}{\sin(\theta_r-\beta)\cos(\theta_r-\omega)} \\ &K_a = \frac{\cos(\rho-\beta)\cos\varphi}{\cos^2\rho} * \frac{\sin\theta_r\cos(\theta_r-\rho)(1-F)}{sin(\theta_r-\beta)\cos(\theta_r-\omega)} \end{aligned} \tag{3}$$

Equation 3 represents the calculation equation for active earth pressure in cohesive soils when assessing slope stability, where K_a denotes the earth pressure coefficient. When applying Equation 3, the critical issue lies in identifying the most dangerous slip plane within the backfill behind the wall and its inclination angle θr. This matter is discussed below, along with several methods for resolving it.

2.3. Method for Determining the Angle of Inclination θ_r of the Most Dangerous Slip Surface

2.3.1. Determine θ_r Based on the Potential Slip Planes within the Slope Body

For certain geotechnical slopes, potential slip surfaces may exist within the slope body due to geological structures, topographical conditions, and other factors. Examples include the most unfavorable stratum in rock slopes following the bedding plane (Figure 3-a), potentially reactivated ancient landslide slip surfaces (Figure 3-b), unfavorable layers or bedrock surfaces in fill slopes, and steep geotechnical layers in embankment slopes. These potential slip surfaces may represent the most hazardous slip surfaces. After identifying potential slip planes in actual engineering projects, one can utilize empirical data, field testing, geological surveys, and other information to determine whether a given plane is the most hazardous slip plane and establish θ_r through theoretical analysis or numerical simulation. Once θ_r is determined, it can be directly substituted into Equation 3 to calculate the earth pressure *Ea*.

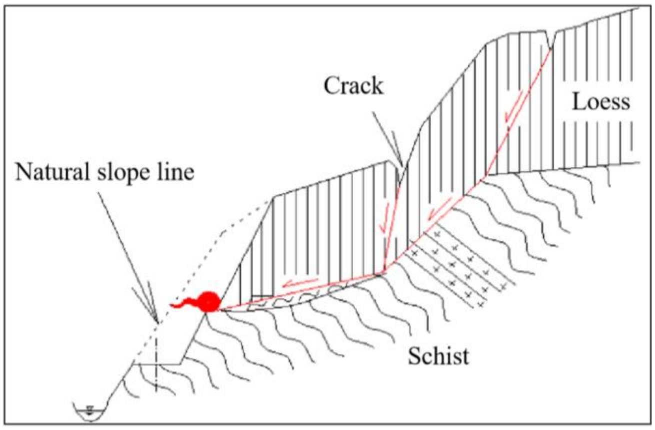

(a) The most unfavorable layer

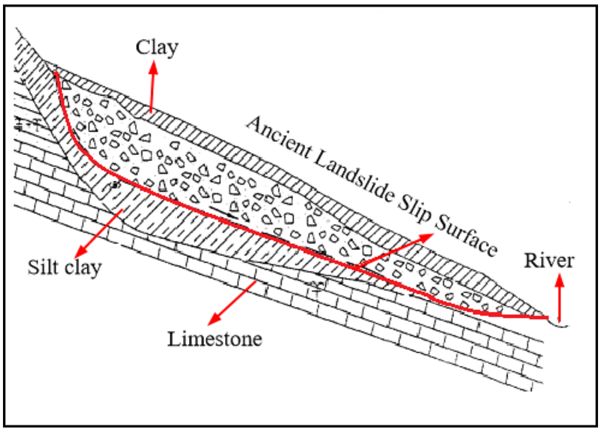

(b) Ancient Landslide Slip Surface

Figure 3. Two cases of potential slip surfaces in slopes

2.4. Determine θ_r Using the Equation

If the slope behind the wall consists of earth or earth-like rock, it may be treated as a continuous homogeneous body. When the wall face is steep or nearly vertical, a plane slip tendency typically develops within the slope. The angle θ_r can be determined using either an iterative or analytical method based on Equation 3.

(1) *Trial Algorithm*

The eight slope parameters in the model shown in Figure 2 can all be determined through design, testing, or geological survey data in actual engineering projects. Once these parameters are established, the earth pressure *E* becomes solely a function of *θ*. Therefore, *Ea* can be calculated using trial-and-error methods. This is illustrated with the following example.

In the model of Figure 2, assuming the eight determined parameter values are H=6m, β=15º, ρ=10º, δ=20º, *C*=10kPa, φ=30º, γ=20kN/m³, and *q*=20kPa, find the value of *θr*. Substituting *E* and *θ* for *Ea* and θ_r in Equation 3, then substituting these parameter values yields: $E = \frac{487.4814 * [sin(\theta-30)cos(\theta-10)-0.1078]}{sin(\theta-15)cos(\theta-60)}$. Substitute different *θ* values into the above equation to calculate the corresponding *E* values. The results can be tabulated (as shown in Table 1) or plotted as a curve of *E* versus *θ* (as shown in Figure 4). This yields $\theta_r \approx 58°$ and $Ea \approx 148$ kN/m.

Table 1. Soil pressure values calculated for different slip plane inclinations

Slope angle *θ* (°)	40	50	55	60	70	80	90
Earth pressure value *E* (kN/m) (rounding to the nearest integer)	52	133	144	145	129	89	25

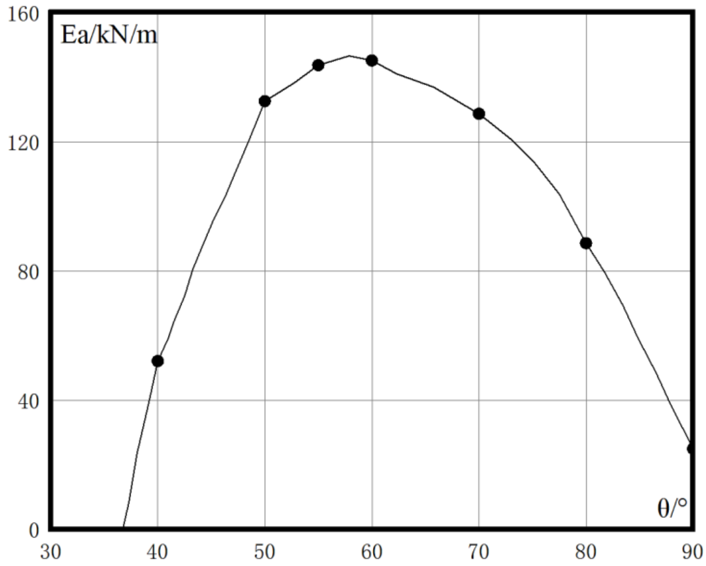

Figure 4. The curve between earth pressure E and inclination angle θ of the sliding surface

(2) ***Analytical Method***

Similarly, substituting E and θ for Ea and θ_r in Equation 3 and solving for their extremum, and setting $\frac{\partial E}{\partial \theta} = 0$ yields the analytical expression for θ_r:

$$\cot\theta_r = -M + \sqrt{M^2 + N}$$
$$M = \frac{\tan\varphi * \tan\omega - tan\beta tan\rho + m(\tan\omega + tan\beta)}{\tan\varphi - tan\beta[1 + \tan\varphi(\tan\omega - tan\rho)] + m(1 - \tan\beta\tan\omega)} \quad (4)$$
$$N = \frac{\tan\omega - [1 + (\tan\varphi - tan\beta)\tan\omega]tan\rho + m(1 - \tan\beta\tan\omega)}{\tan\varphi - tan\beta[1 + \tan\varphi(\tan\omega - tan\rho)] + m(1 - \tan\beta\tan\omega)}$$

After determining θ_r, substitute it into Equation 3 to obtain Ea. For example, substituting the parameter values used in the trial method into Equation 4 yields θ_r=58.5°. Substituting θ_r into Equation 3 calculates K_a=0.311, and the final calculation gives Ea=147.60 kN/m, which is consistent with the result from the trial method. In engineering practice, these two methods can be integrated into a simple software tool to facilitate the determination of θ_r.

3. Influence of Slope Stability Behind the Wall on Earth Pressure

Once θ_r within the slope behind the wall is determined, the slope stability significantly influences the earth pressure. The safety factor can be calculated using Equation 2, where $\frac{W\sin\theta_r\cos\varphi}{\cos(\theta_r-\omega)}$ represents the total pressure exerted on the wall by the gravitational load W, and $\frac{W\sin\theta_r\cos\varphi * F}{\cos(\theta_r-\omega)}$ represents the reduction in total pressure due to the enhanced stability of the slope behind the wall provided by the two strength parameters of cohesive soil. The greater the value of F, the more stable the slope behind the wall becomes, leading to a greater reduction in total pressure and enhancing the wall's safety. When F<1, the slope behind the wall tends to slide and compress the wall due to instability. The wall provides an equal amount of resistance to maintain equilibrium in the wall-soil system. At this point, the earth pressure Ea calculated from Equation 2 is positive, indicating the wall is subjected to corresponding earth pressure. When F≥1, the slope behind the wall is in a state of critical stability or stability. Even without the wall's obstruction, the slope will not slip or become unstable, so the wall is not subjected to earth pressure. The stability level of the slope behind the wall can serve as a reference for the rational design of retaining walls.

To further illustrate the effect of F on Ea, consider the example from Section 2.3.2. In this example, θ_r=58.5° has been determined. From Equation 2, F=0.5741<1, indicating that the slope behind the wall tends to slide along a slip plane inclined at 58.5°. At this point, Ea calculated using Equation 2 is $Ea=346.6217*(1-F)$ =147.60 kN/m. If the bond strength C value in this example is increased from 10 kPa to 40 kPa, θ_r=66° is obtained using Equation 4. The resulting F=1.11>1 from Equation 2. Calculating Ea using Equation 2: $Ea=288.693*(1-F)$ =-31.76kN/m. This indicates the slope behind the wall is stable and can be designed for slope protection.

4. Factors Affecting Earth Pressure Calculations

4.1. Earth Pressure Coefficient K_a

The Equation 3 for the earth pressure coefficient K_a can be rewritten as:

$$K_a = K_{a1} - K_{a2}$$
$$K_{a1} = \frac{\cos(\rho-\beta)}{\cos^2\rho} * \frac{\sin(\theta_r-\varphi)\cos(\theta_r-\rho)}{\sin(\theta_r-\beta)\cos(\theta_r-\omega)} \tag{5}$$
$$K_{a2} = \frac{m\cos\rho\cos\varphi * K_{a1}}{\sin(\theta_r-\varphi)\cos(\theta_r-\rho)}$$

where, K_{a1} is Sand pressure coefficient; K_{a2} is Clay pressure coefficient.

Equation 5 indicates that the earth pressure coefficient K_a for cohesive soils is composed of two components: K_{a_1} and K_{a_2}, which are derived from the sandiness index φ and cohesion index C. The presence of C enhances slope stability, resulting in K_{a_2} being negative and K_{a_1} being greater than K_a. For quantitative illustration, substitute the parameter values used in Example 1.3.2 into Equation 5. Calculation results: K_{a1}=0.472, K_{a2}=0.1609, K_{a1}/K_{a2}=0.341. If the cohesion parameter C=0 in Equation 3, then m=0, allowing its application to sandy soil pressure calculations. The soil pressure coefficient is K_{a1}, but θ_r must be recalculated using Equation 4. The resulting calculations verify consistency with the classical Coulomb soil pressure equation [22].

Regarding the distribution of earth pressure stress on the wall surface, let $\gamma H+2qn=q_a$, which represents the equivalent vertical stress generated by the soil's self-weight and load q. Equation 3 then becomes:

$$E_a = \frac{H}{2} * q_a K_a = \frac{H}{2} * q_a K_{a1} - H * q_c K_{a1} \tag{3A}$$

In the equation: $q_c = \frac{\cos\rho\cos\varphi * C}{\sin(\theta_r-\varphi)\cos(\theta_r-\rho)}$, this represents the equivalent vertical stress generated by the bond strength. Since the slip plane is assumed to be planar, Equation 3A indicates that the distribution of earth pressure on the wall surface is also linear. *Ea* represents the earth pressure value corresponding to the superposition of a triangular distribution and a rectangular distribution.

4.2. Wall-soil Separation Causing Cracks

Some literature suggests that displacement caused by earth pressure may lead to separation between the upper soil layer and the wall surface, resulting in cracks. This assertion warrants further discussion. When the wall and soil mass are in a state of static equilibrium at the limit state, the wall provides a resisting force equal to *Ea*. With no displacement of the wall, no cracks exist. Otherwise, displacement of the wall occurs, and at this point, studying the effect of cracks on earth pressure becomes meaningless. The wall-soil model in Figure 5-a is used below to further illustrate this point.

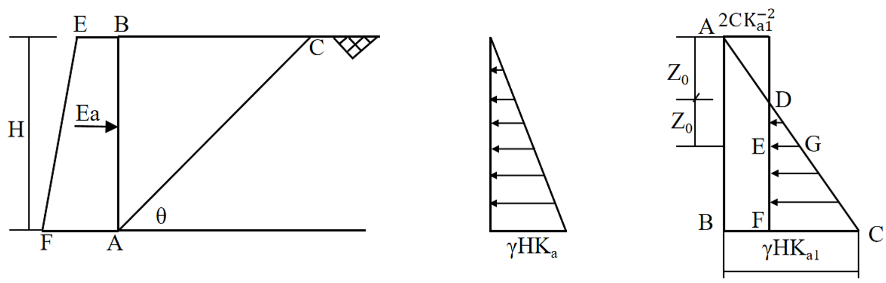

(a) Wall soil body model (b) Stress distribution (c) Stress distribution

Figure 5. The slope model and earth pressure stress distribution

In this model, the walls are smooth and vertical, while the slope surface is horizontal and unloaded. The corresponding slope parameters in Equation 3 are: β=0, ρ=0, δ=0, q=0. Here, n=1, $m=2C/(\gamma H)$, and $\omega=\varphi$. First, calculate θ_r. From Equation 4, $M=\tan\varphi$ and N=1. Substituting into Equation 4, $\cot\theta r=(1-\sin\varphi)/\cos\varphi$, yielding $\theta_r=45°+\varphi/2$. Next, calculate the earth pressure coefficient K_a. From Equation 5, $K_{a_1}=\tan2(45°-\varphi/2)$. In Equation 3A, $q_a=\gamma H$ and $q_c=2C/K_{a_1}{}^{1/2}$, transforming Equation 3A to:

$$E_a = \frac{H}{2} * \gamma H K_a \tag{3B}$$

$$E_a = \frac{H}{2} * \gamma H K_{a1} - 2C\sqrt{K_{a1}} * H \tag{3C}$$

At this point, the distribution of earth pressure on the wall surface should be linear. If calculated using Equation 3B, the earth pressure distribution takes the form shown in Figure 5-b, which is a triangular distribution with base K_a and height *H*. Calculating using Equation 3C yields an earth pressure distribution as shown in Figure 5-c. This represents the sum of a triangular distribution with base $K_{a,}$ and height *H*, and a rectangular distribution with base $2C\sqrt{K_{a1}}$ and height *H*. The combined result forms a trapezoidal distribution EFCG. Based on the stress distribution diagram in Figure 5-c, the separation of soil at height Z_0 in the upper wall section from the wall surface, resulting in cracks, is attributed to wall displacement. Therefore, it is recommended to adopt the earth pressure corresponding to triangle DFC as the final earth pressure value: $E_a = \frac{\gamma H^2}{2} * K_{a1} - 2CH\sqrt{K_{a1}} + \frac{2C^2}{\gamma}$.

According to this equation, when the cohesion $C > \frac{\gamma H\sqrt{K_{a1}}}{2}$, *Ea* increases rapidly with increasing *C* value, which is inconsistent with the earth pressure characteristics of cohesive soils. However, when calculated using Equation 3C, *Ea* decreases as *C* increases when $C < \frac{\gamma H\sqrt{K_{a1}}}{4}$; when $C \geq \frac{\gamma H\sqrt{K_{a1}}}{4}$, *Ea* becomes zero or negative, which aligns with the characteristics of cohesive soils. Therefore, for wall-soil models such as the one shown in Figure 5-a, it is recommended to use Equations 3B or 3C to calculate earth pressure.

4.3. Influence of Slope Parameters on Earth Pressure

Equation 3 is a function of eight slope parameters (*H, β, ρ, δ, C, φ, γ, q*), and changes in any parameter will affect the *Ea* value. Understanding how these parameters influence *Ea* provides a reference for selecting appropriate parameter values in engineering design. The influence of *θ* has been discussed earlier, and the equation for calculating θ_r (Equation 4) has been derived. When examining the effects of these eight parameters, we will continue to employ the single-factor method used in the analysis of *θ*'s influence. This involves treating a specific parameter as the variable of interest while keeping all other parameters constant. First, determine the most dangerous slip surface within the slope and its inclination angle θ_r. Based on this, discuss the influence of these parameters. For this example, the eight parameters and θ_r retain the values from the example in Section 2.3.2: θ_r=58.5°, *H*=6m, *β*=15°, *ρ*=10°, *δ*=20°, *C*=10kPa, *φ*=30°, *γ*=20kN/m^3, and *q*=20kPa.

(1) Effect of wall height *H*

Let *H* be the variable, after calculation, Equation 3 becomes:

$$E_a = \frac{cos(\rho-\beta)*cos(\theta_r-\rho)sin(\theta_r-\varphi)*\gamma}{2cos^2\rho sin(\theta_r-\beta)cos(\theta_r-\omega)} * H[H-A] \tag{6}$$

In the equation: $A = \frac{2Ccos\rho cos\varphi}{\gamma * cos(\theta_r-\rho)sin(\theta_r-\varphi)} - \frac{2q\eta}{\gamma}$, Substituting the known parameter values into the above equation yields the quantitative relationship between *Ea* and *H*: *Ea=4.7196H(H-0.7877).*

The resulting curve of *Ea* versus *H* is shown in Figure 6, where *Ea* increases non-linearly with increasing *H*. In practical engineering applications, Equation 6 can be used to select a reasonable wall height to control the earth pressure value.

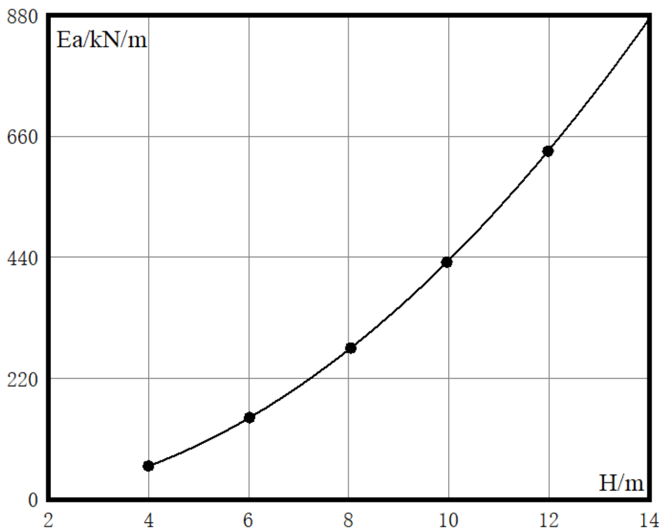

Figure 6. The curve of *Ea* and *H*

(2) Effect of wall surface inclination angle β

Setting β as the variable, after calculation, Equation 3 becomes:

$$E_a = \frac{BHcos(\theta_r-\rho)sin(\theta_r-\varphi)tan\rho}{2cos\rho cos(\theta_r-\omega)cos\theta_r} * \frac{\frac{2q}{Btan\rho}+\frac{1}{tan\rho}+tan}{tan\theta_r-tan\beta} \quad (7)$$

In the equation: $B = \gamma H - \frac{2Ccos\rho cos\varphi}{cos(\theta_r-\rho)sin(\theta_r-\varphi)}$, Substituting the known parameter values into the above equation yields the quantitative relationship between *Ea* and β: $E_a = \frac{21.4762(9.1058+tan\beta)}{1.6319-tan\beta}$.

The resulting curve of *Ea* versus β is shown in Figure 7, where *Ea* increases non-linearly with increasing β. It is worth noting that larger β angles can cause surface slope instability.

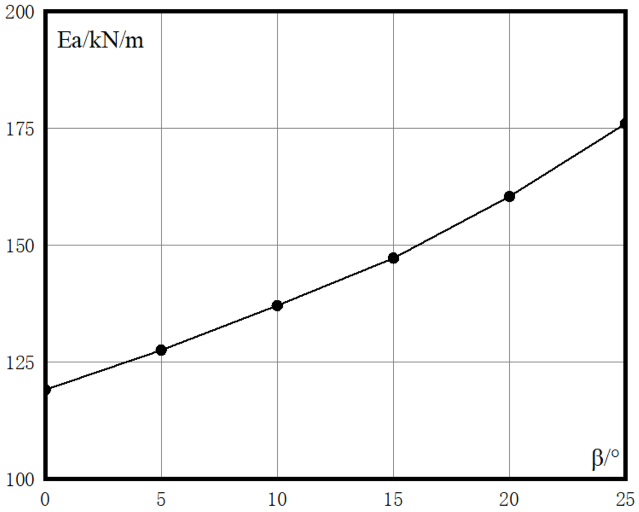

Figure 7. The curve of *Ea* and *β*

(3) Effect of wall inclination angle ρ

Setting ρ as the variable, after calculation, Equation 3 becomes:

$$E_a = \frac{\gamma H^2 sin\beta sin(\theta_r-\varphi)sin\theta_r}{2sin(\theta_r-\beta)sin(\theta_r-\varphi-\delta)} * \frac{(D+tan\rho)(F+tan\rho)}{cos\rho[cot(\theta_r-\varphi-\delta)+tan\rho]} \quad (8)$$

In the equation: $D = \frac{\gamma H+2q}{\gamma Htan\beta}$, $F = cot\theta_r - \frac{mcos\varphi}{sin(\theta_r-\varphi)sin\theta_r}$, Substituting the known parameter values into the above equation yields the quantitative relationship between *Ea* and ρ: $E_a = \frac{372.5745*(4.9761+tan\rho)(0.3437+tan\rho)}{cos\rho(6.6912+tan\rho)}$.

The resulting curve of *Ea* versus ρ is shown in Figure 8, where *Ea* increases non-linearly with increasing β. It is worth noting that larger β angles can cause surface slope instability. As ρ increases, *Ea* increases. When the wall is inclined and the angle of inclination ρ is less than arctan(-0.3437) = -18.97°, *Ea* becomes negative, indicating the stability of the slope behind the wall.

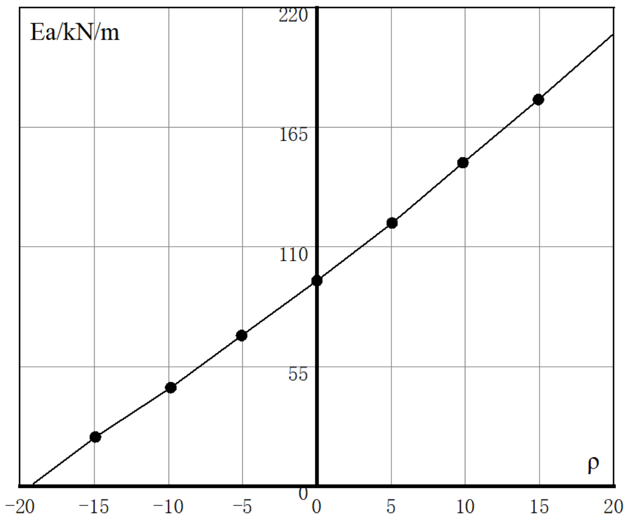

Figure 8. The curve of *Ea* and *ρ*

(4) Effect of the friction angle δ between the soil and the wall

When δ is set as a variable, this variable appears only in the $cos(\theta_r-\omega)$ term of Equation 3, after calculation, Equation 3 becomes: $E_a = \frac{147.5659}{cos(18.5°-\delta)}$.

The resulting curve of *Ea* versus δ is shown in Figure 9, when δ=18.5°, Ea reaches its minimum value.

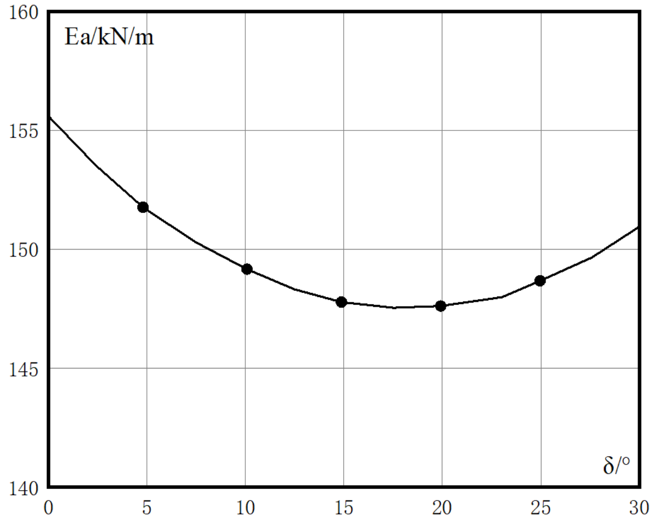

Figure 9.The curve of *Ea* and *δ*

(5) Effect of soil cohesion *C*

When C is set as a variable, this variable appears only in the term m=2C/(γH+2qn) of Equation 3, after calculation, Equation 3 becomes: *Ea=7.637(29.3321-C).*

The resulting curve of *Ea* versus *C* is shown in Figure 10. As *C* increases, *Ea* decreases linearly. When *C* exceeds 29.3321 kPa, *Ea* becomes negative, indicating that the slope behind the wall is stable and the wall is not subjected to earth pressure.

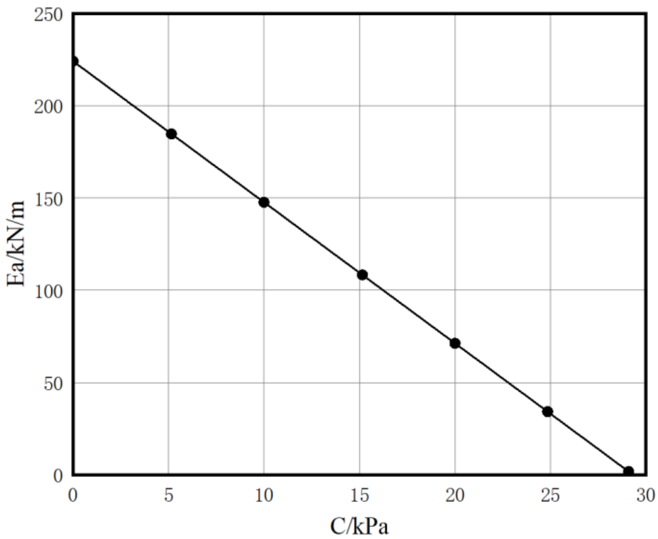

Figure 10. The curve of *Ea* and *C*

(6) Effect of internal friction angle φ of soil

Setting φ as the variable, substituting the known parameter values into Equation 3 yields the relationship between *Ea* and φ:

$$E_a = \frac{469.2566[sin(\theta_r-\varphi)-0.1879cos\varphi]}{cos(28.5-\varphi)} \tag{9}$$

The resulting curve of *Ea* versus φ is shown in Figure 11. As φ increases, *Ea* decreases approximately linearly.

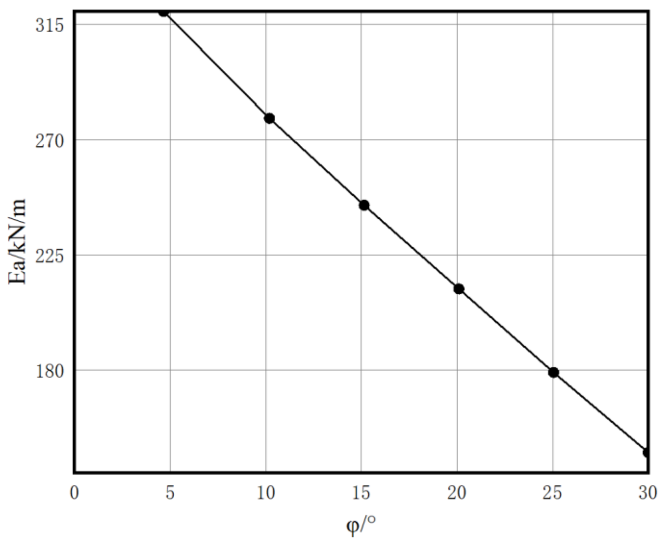

Figure 11. The curve of *Ea* and *φ*

(7) Effect of soil weight γ

Setting γ as the variable, after calculation, Equation 3 becomes:

$$E_a = \frac{H^2 cos(\rho-\beta)cos(\theta_r-\rho)sin(\theta_r-\varphi)}{2cos^2\rho sin(\theta_r-\beta)cos(\theta_r-\omega)}[\gamma - G] \tag{10}$$

In the equation: $G = \frac{2Ccos\rho cos\varphi}{Hcos(\theta_r-\rho)sin(\theta_r-\varphi)} - \frac{2qn}{H}$, Substituting the known parameter values into Equation 10 yields the relationship between *Ea* and γ: *Ea=8.4953(γ-2.6255).*

The resulting curve of *Ea* versus γ is shown in Figure 12. As γ increases, *Ea* increases linearly:

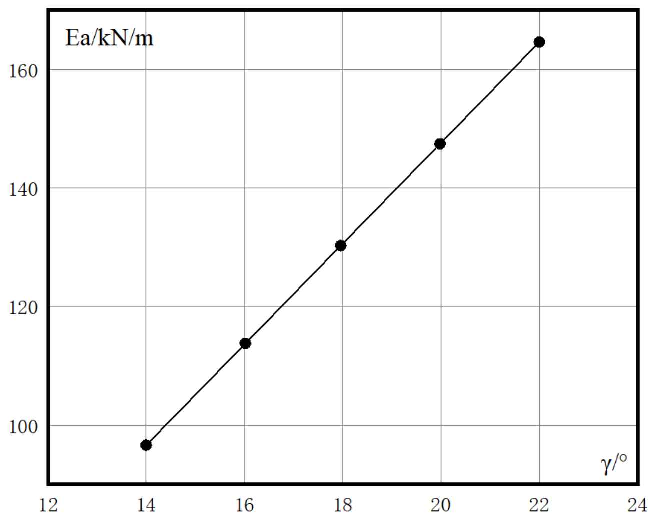

Figure 12. The curve of *Ea* and *γ*

(8) Effect of surface load *q*

Setting *q* as the variable, after calculation, Equation 3 becomes:

$$E_a = \frac{nHcos(\rho-\beta)cos(\theta_r-\rho)sin(\theta_r-\varphi)}{cos^2\rho sin(\theta_r-\beta)cos(\theta_r-\omega)}[q + H] \tag{11}$$

In the equation: $H = \frac{\gamma H}{2n} - \frac{C*cos\rho cos\varphi}{ncos(\theta_r-\rho)sin(\theta_r-\varphi)}$, Substituting the known parameter values into Equation 11 yields the relationship between *Ea* and *q*: *Ea=2.704(q+34.5852).*

The resulting curve of *Ea* versus *q* is shown in Figure 13. As *q* increases, *Ea* increases linearly.

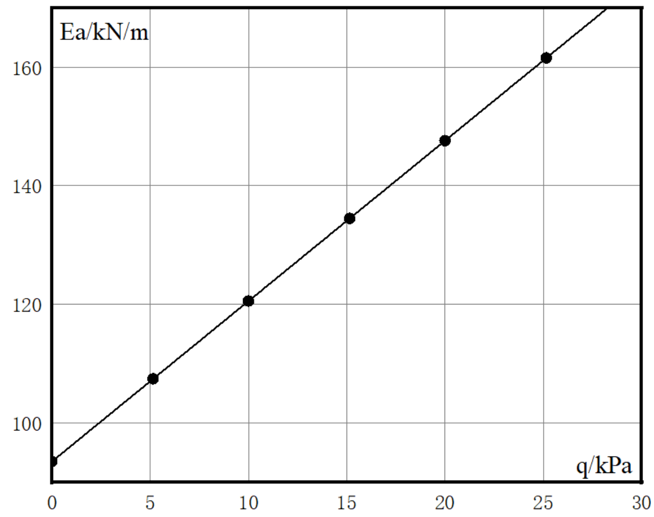

Figure 13. The curve of *Ea* and *q*

5. Application of Equation 3

Figure 2 model involves eight parameters. Assigning different values to each parameter yields distinct wall-soil system models, and Equation 3 is also applicable for calculating earth pressure in these models. When $C=0$, this equation is also suitable for calculating earth pressure in sandy soils. The general calculation steps when using Equation 3 are as follows: ① Determine the model and parameters based on the project conditions; ② Identify the most dangerous slip surface and its inclination angle θ_r using the method described in Section 2.3; ③ Calculate the safety factor *F* for the slope behind the wall using Equation 2; ④ If $F<1$, calculate *Ea* using Equation 3. If $F\geq 1$, terminate the calculation, as the calculated *Ea* will be zero or negative. The following example provides further illustration.

(1) Figure 14 presents a wall-soil system model established based on a specific project. The crest ground level is horizontal, with the inclined wall surface having a slope ratio of *1:0.2*. The parameters required for Equation 3, determined through design and testing, are: H=8m, β=0, ρ=-11.3°, δ=15°, C=15kPa, φ=24°, γ=19kN/m³, q=10kPa. Calculate the earth pressure *Ea*

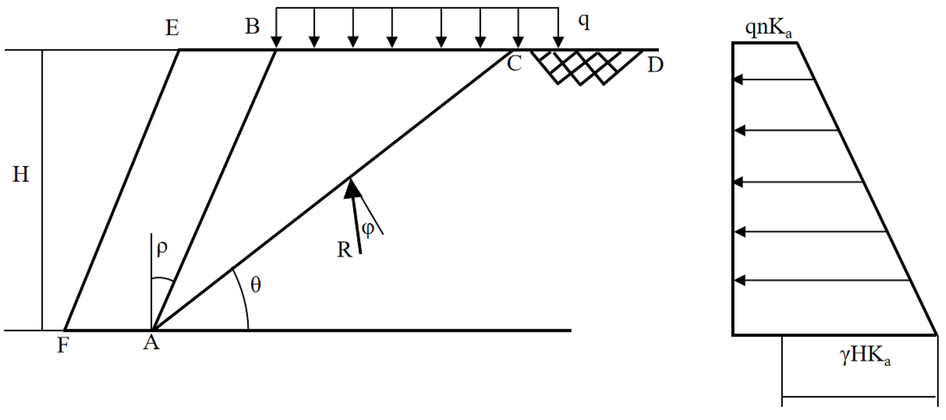

Figure 14. Wall-soil system model and the stress distribution

① Calculate using Equation 3

At this point, the influence coefficient q is n=1, the cohesion influence coefficient m=0.1744, and ω=27.7°. The wall surface is steep, and the slope behind the wall is a quasi-soil slope, satisfying the conditions for plane sliding instability. The inclination angle θ_r of the most dangerous sliding surface can be determined using Equation 4. From Equation 4: $M=tan27.7°$, N=1.5266, $cot\theta_r$=0.8175, θ_r=50.7°. Calculating the safety factor F for the slope behind the wall using Equation 2 yields F=0.8352. Calculating the earth pressure coefficient K_a using Equation 3 yields K_a=0.0783, and the earth pressure value Ea=53.87kN/m.

② Calculate according to the standard.

According to Section 6.2.3 of the Technical Specifications for Engineering of Building Slopes (GB 50330-2013): Based on the plane slip plane assumption, the resultant active earth pressure can be calculated using the following equation:

$$E_a = \frac{1}{2} * \gamma H^2 K_a$$

$$K_a = \frac{sin(\alpha+\beta)}{sin^2\alpha sin^2(\alpha+\beta-\varphi-\rho)} * \left\{ \begin{array}{c} K_q[sin(\alpha+\delta)sin(\alpha-\delta)+sin(\varphi+\delta)sin(\varphi-\beta)] \\ +2\eta sin\alpha cos\varphi cos(\alpha+\beta-\varphi-\delta) \\ -2\sqrt{K_q sin(\alpha+\beta)sin(\varphi-\beta)+\eta sin\alpha cos\varphi} \\ \times\sqrt{K_q sin(\alpha-\delta)sin(\varphi+\delta)+\eta sin\alpha cos\varphi} \end{array} \right\} \tag{11}$$

$$K_q = 1 + \frac{2q sin\alpha cos\beta}{\gamma H sin(\alpha+\beta)}$$

$$\eta = \frac{2C}{\gamma H}$$

When calculating earth pressure according to the standard (Equation 11), with α=90°-ρ=101.3° and β=0°, and all other parameters unchanged, substituting these values into Equation 11 yields: η=30/(19×8)=0.1974, K_q=1.1316, K_a=0.0886, *Ea*=53.87kN/m. The earth pressure values obtained from both methods are identical.

(2) The model and parameters from Figure 14 are still used, but the wall is backed by a sandy soil slope, so the cohesion parameter *C* in the parameters is set to 0. The earth pressure *Ea* on the wall is calculated accordingly.

① Calculate using Equation 3

At this point, *n*=1, $m=2C/(\gamma h+2qn)$ =0, and ω=27.7°. The conditions for plane slip failure are still satisfied. First, determine the inclination angle θ_r of the most dangerous slip plane. Substituting all parameters into Equation 4 yields: $cot\theta_r$=0.8813， θ_r=48.6°. Next, using Equation 2, the safety factor *F* for the slope behind the retaining wall is calculated as *F*=0.3925. Finally, applying Equation 3, the earth pressure value *Ea* is determined to be *Ea*=209.03kN/m.

② Calculate according to the standard.

When calculating earth pressure according to the standard (Equation 11), with $\eta=2C/(\gamma H)$=0, and all other parameters unchanged, substituting these values into Equation 11 yields: K_a=0.3438, *Ea*=209.03kN/m. The earth pressure values obtained from both methods are identical.

6. Conclusions

A large number of engineering projects have shown that the stability of cohesive soil slopes behind retaining walls has a significant influence on earth pressure. To clarify how slope stability affects earth pressure, this study investigates the influence of cohesive soil slope stability on the pressure acting behind retaining walls. First, the interaction mechanism between the wall and the slope was analyzed to better understand the mechanical behavior of clayey soil pressure. Second, based on the assumptions of planar slip failure and limit equilibrium conditions, an active earth pressure calculation equation for cohesive soil that considers slope stability was proposed. Third, using the proposed equation, the influence of various slope parameters on earth pressure was analyzed, and a method for determining the most critical slip surface and slope inclination angle was introduced. Finally, the validity of the proposed equation was verified through numerous numerical examples. The main findings are summarized as follows:

- The interaction mechanism between the retaining wall and the slope was analyzed to clarify the mechanical behavior of clayey soil pressure. Based on the assumptions of planar slip failure and limit equilibrium conditions, an active earth pressure equation for cohesive soil considering slope stability was developed.
- Using the proposed equation, the influence of slope stability and various slope parameters on earth pressure was analyzed. In addition, a method was proposed for determining the most critical slip surface and slope inclination angle.
- To verify and apply the proposed equation, several case studies on earth pressure acting on retaining walls were conducted. Earth pressure values were calculated using both the proposed equation and the standard code-based equation. A comparison of the results showed strong agreement between the two methods, confirming the validity of the proposed equation.

These findings provide a simple and practical approach for calculating earth pressure in cohesive or sandy soils and offer a useful reference for improving the understanding of the complex mechanical behavior of earth pressure in cohesive soils.

7. Declarations

7.1. Author Contributions

Conceptualization, T.Y. and S.W.W.; methodology, D.P.Z. and S.W.W.; validation, H.Q.T.; formal analysis, Z.Z.; writing—original draft preparation, D.P.Z. and S.W.W.; writing—review and editing, T.Y. and S.W.W.; supervision, T.Y. All authors have read and agreed to the published version of the manuscript.

7.2. Data Availability Statement

The data presented in this study are available on request from the corresponding author.

7.3. Funding

This research was funded by the Natural Science Foundation of Sichuan Province (2025ZNSFSC0305): Intelligent inversion analysis of landslide stability based on point safety coefficient.

7.4. Conflicts of Interest

The authors declare no conflict of interest.

8. References

[1] Gao D. Z. (1998). Soil Mechanics and Foundation Engineering. China Architecture and Building Press, Beijing, China.

[2] Chen, J., Qian, B., & Yu, M. (2024). Active Earth Pressure Calculation for a Translational Retaining Wall Considering the Influence of Basement Inverse Slope. International Journal of Geomechanics, 24(8). doi:10.1061/ijgnai.gmeng-9723.

[3] Ma, Q., Chen, Z., Zheng, J., Liu, Y., & Zeng, G. (2024). Earth Pressure Calculation of High Fill Culvert Considering Inclination of Soil Column Interface. Iranian Journal of Science and Technology - Transactions of Civil Engineering, 48(5), 3573–3590. doi:10.1007/s40996-024-01416-7.

[4] Deng, B., Yang, M. H., Wang, D. X., & Fan, J. W. (2022). Failure mode and active earth pressure calculation of unsaturated soil behind rigid retaining wall. Yantu Lixue/Rock and Soil Mechanics, 43(9), 2371–2382. doi:10.16285/j.rsm.2021.1924.

[5] Tang, Y., & Chen, J. (2020). New Approach for Active Earth Pressure Calculation on Rigid Retaining Walls with Cohesive Backfill. Soil Mechanics and Foundation Engineering, 57(4), 288–295. doi:10.1007/s11204-020-09668-x.

[6] Peng, M. X. (2009). Coulumb's unified solution of active earth pressure on retaining wall. Yantu Lixue/Rock and Soil Mechanics, 30(2), 379–386. doi:10.16285/j.rsm.2009.02.054.

[7] Fang, W., Cui, Y., & Liu, S. (2025). Nonlinear Rankine pressure of unsaturated soil under transient infiltration. Canadian Geotechnical Journal, 62, 1–16. doi:10.1139/cgj-2024-0408.

[8] Guo, D., Zhang, M., Liu, Y., & Wu, Y. (2025). Unsaturated Rankine soil pressure analysis under unsteady seepage. Harbin Gongye Daxue Xuebao/Journal of Harbin Institute of Technology, 57(11), 45–52. doi:10.11918/202401053.

[9] Tracy, F. T., & Vahedifard, F. (2025). Analytical solutions for coupled hydromechanical modeling of lateral earth pressures in unsaturated soils. Computers and Geotechnics, 179. doi:10.1016/j.compgeo.2024.107038.

[10] Chen, F. Q., Chen, H. B., Wu, Y. X., Zhang, D. B., & Lin, Y. J. (2023). Numerical and analytical study on active earth pressure against inverted T-type retaining walls rotating about the base. Acta Geotechnica, 18(4), 2195–2216. doi:10.1007/s11440-022-01723-1.

[11] Zhu, D. Y., Qian, Q. H., & Lee, C. F. (2001). Active and passive critical slip fields for cohesionless soils and calculation of lateral earth pressures. Géotechnique, 51(5), 407-423. doi:10.1680/geot.2001.51.5.407.

[12] GB 50330-2013. (2013). Technical code for building slope engineering. Ministry of Housing and Urban-Rural Development, Beijing, China. (In Chinese).

[13] Terzaghi, K. (1943). Theoretical Soil Mechanics. John Wiley and Sons, Hoboken, United States. doi:10.1002/9780470172766.

[14] Chen, Z., Li, S., Xue, Y., Ma, L., Lu, Y., & Yao, Z. (2026). Earth Pressure Calculation Method for Shallow-Buried Loess Tunnels Considering Support and Size Effects. International Journal of Geomechanics, 26(3). doi:10.1061/ijgnai.gmeng-12074.

[15] Hu, W., Zeng, Y., Zhu, X., & Hu, T. (2023). Determination of Passive Earth Pressure on a Cantilever Retaining Wall in a Narrow Foundation Pit Based on Logarithmic Spiral Sliding Surface. International Journal of Geomechanics, 23(8), 8516. doi:10.1061/ijgnai.gmeng-8516.

[16] Mazindrani, Z. H., & Ganjali, M. H. (1997). Lateral Earth Pressure Problem of Cohesive Backfill with Inclined Surface. Journal of Geotechnical and Geoenvironmental Engineering, 123(2), 110–112. doi:10.1061/(asce)1090-0241(1997)123:2(110).

[17] Fang, W., Wu, R.-F., Cui, Y.-J., & Liu, S. (2026). Rankine Active Earth Pressure of Unsaturated Soil Based on the Envelope Shell Model. International Journal of Geomechanics, 26(3), 04025364. doi:10.1061/ijgnai.gmeng-12524.

[18] Liang, L., Xu, C., Fan, X., & Chen, Q. (2023). Hyperbolic stress-strain behaviour of sandy soil under plane strain unloading condition and its application on predicting displacement-dependent active earth pressure. Computers and Geotechnics, 155, 105219. doi:10.1016/j.compgeo.2022.105219.

[19] Fan, L., Zheng, Z., Peng, S., Zhou, J., Shen, T., Wan, H., & Ma, H. (2023). An improved method of active earth pressure on rigid retaining wall under movement modes considering arching effects. International Journal for Numerical and Analytical Methods in Geomechanics, 47(3), 410–424. doi:10.1002/nag.3475.

[20] Que, Y., Long, C., & Chen, F. (2023). Slip Line Solution for Active Earth Pressure of Retaining Walls with Relief Shelves Subjected to Base Rotation. International Journal of Geomechanics, 23(10), 04023176. doi:10.1061/ijgnai.gmeng-8540.

[21] Lai, F., Zhang, N., Liu, S., & Yang, D. (2022). A generalised analytical framework for active earth pressure on retaining walls with narrow soil. Geotechnique, 74(11), 1127–1142. doi:10.1680/jgeot.21.00305.

[22] Pantelidis, L. (2019). The generalized coefficients of earth pressure: a unified approach. Applied Sciences, 9(24), 5291. doi:10.3390/app9245291.